Acta Crystallographica Section F
Structural Biology and Crystallization Communications
ISSN 1744-3091

Purification, crystallization and preliminary X-ray crystallographic analysis of the receiver and stalk domains (PA3346RS) of the response regulator PA3346 from *Pseudomonas aeruginosa* PAO1

Pei-Hsiu Wu,[a,b] Jye-Jin Hsu,[c] Ting-Wei Chiang,[a,d] Yin-Cheng Hsieh,[a] Hwan-You Chang,[c] Shou-Lin Chang[b]* and Chun-Jung Chen[a,d,e]*

[a]Life Science Group, Scientific Research Division, National Synchrotron Radiation Research Center, Hsinchu 30076, Taiwan, [b]Institute of Bioinformatics and Structural Biology, National Tsing-Hua University, Hsinchu 30013, Taiwan, [c]Institute of Molecular Medicine, National Tsing-Hua University, Hsinchu 30013, Taiwan, [d]Department of Physics, National Tsing-Hua University, Hsinchu 30013, Taiwan, and [e]Institute of Biotechnology, National Cheng-Kung University, Tainan 701, Taiwan

Correspondence e-mail: slchang@life.nthu.edu.tw, cjchen@nsrrc.org.tw

Received 12 April 2011
Accepted 18 June 2011

The regulatory domain (PA3346RS), comprising the receiver and stalk domains, of the response regulator PA3346 requires phosphorylation for activation with magnesium ions as cofactors in order to modulate the downstream protein phosphatase activity for the regulation of swarming motility in *Pseudomonas aeruginosa* PAO1. Fusion-tagged recombinant PA3346RS of total molecular mass 25.3 kDa has been overexpressed in *Escherichia coli*, purified using Ni^{2+}–NTA and Q-Sepharose ion-exchange columns and crystallized using the hanging-drop vapour-diffusion method. X-ray diffraction data were collected from PA3346RS crystals to 2.0 Å resolution. The crystal belonged to space group $P4_1$ or $P4_3$, with unit-cell parameters a = 82.38, c = 73.34 Å. Preliminary analysis indicated the presence of a dimer of PA3346RS in the asymmetric unit, with a solvent content of 48.6%.

1. Introduction

Two-component regulatory systems (TCSs) play pivotal roles in the adaptation and pathogenesis of bacteria. Hybrid TCSs in bacterial and some eukaryotic organisms are utilized for the reception of responses to environmental stimuli and are composed of a membrane-associated ITR-type sensor histidine kinase (HK) domain, a histidine-containing phosphotransfer (Hpt) domain and a cytoplasmic response regulator (RR) domain (Varughese, 2002; West & Stock, 2001). The ITR-type sensor kinases, thus named because they include **i**nput, **t**ransmitter and **r**eceiver-like domains, relay phosphoryl groups to the cognate RR through an Hpt module protein, as shown in Fig. 1.

Pseudomonas aeruginosa is a versatile Gram-negative pathogen that causes many acute and chronic infections, especially in cystic fibrosis patients (Stover *et al.*, 2000; Rodrigue *et al.*, 2000). A swarming-regulating TCS in *P. aeruginosa* PAO1 has been elucidated which comprises four orphan sensor kinases PA1611, PA1976, PA2824 and PA4856, one phosphotransfer protein HptB (PA3345) and one specific response regulator (RR) PA3346 (Hsu *et al.*, 2008). PA3346 is a novel protein phosphatase comprising an N-terminal receiver domain (REC), a stalk linker (S), a Ser/Thr protein phosphatase domain in the middle portion and a C-terminal ATP-binding domain. The Ser/Thr protein phosphatase domain is a homologue of RsbU from *Bacillus subtilis* and has been classified into the manganese-dependent PP2C family (Shi, 2004). Phosphorylation at the REC domain activates the phosphatase activity and could lead to dephosphorylation of the putative antisigma antagonist PA3347, a

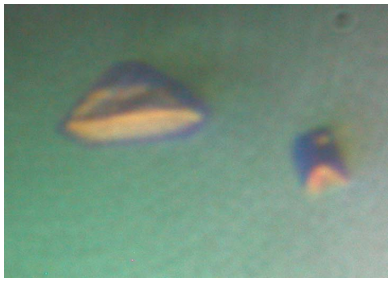

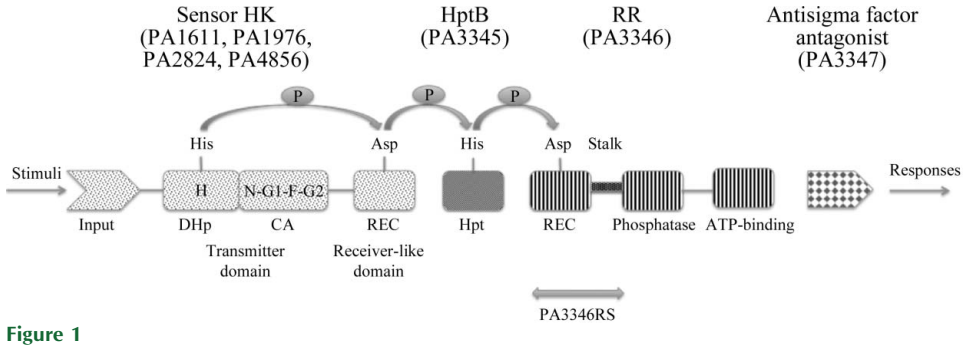

Figure 1
Hybrid two-component regulatory system.

homologue of RsbV from *B. subtilis* (Searls *et al.*, 2004; Wise & Price, 1995). The REC of PA3346 (PA3346REC) thus functions as a switch that controls the mechanism of downstream activation, including swarming phenotype and biofilm formation (Hsu *et al.*, 2008; Lin *et al.*, 2006).

The N-terminal regulatory region of PA3346 (PA3346RS), comprising the REC and stalk (S) domains, is subjected to phosphorylation and requires magnesium ions (Mg^{2+}) as cofactors to modulate the downstream phosphatase activity (Bourret, 2010). Three structures containing the upstream receiver-like domain have been determined, including the signal receiver domain from *Syntrophus aciditrophicus* (Y. Patskovsky, R. Toro, C. Morano, J. Freeman, S. Hu, J. M. Sauder, S. K. Burley & S. C. Almo, unpublished results; PDB entry 3gt7), the receiver domain Spo0F in complex with the Hpt Spo0B from *B. subtilis* (Zapf *et al.*, 2000; Varughese *et al.*, 2006) and the receiver domain SLN1-R1 with the cognate Hpt YPD1 from *Saccharomyces cerevisiae* (Xu *et al.*, 2003). For downstream response regulators, only two dimeric structures of RssB (PA2798) from *P. aeruginosa* (L. Levchenko, R. A. Grant, R. T. Sauer & T. A. Baker, unpublished results; PDB entry 3eq2) and WspR (PA3702) from *P. aeruginosa* PAO1 (De *et al.*, 2008; PDB entry 3bre) are available. RssB is a 394-amino-acid ClpX adaptor protein involving the SpoIIE domain that regulates σ^S (Bougdour *et al.*, 2006), whereas the diguanylate cyclase WspR is a conserved 446-amino-acid GGDEF-domain-containing response regulator from *P. aeruginosa* PAO1 (De *et al.*, 2008).

Multiple sequence alignments of the REC and S domains of PA3346 and the two related proteins revealed low sequence identities of 30.1 and 21.6% between the N-terminal region of PA3346 (PA3346N; residues 1–185) and RssB (residues 1–166) and WspR (residues 1–176), respectively, with 8.4 and 6.8% gaps. Moreover, the stalk of PA3346N contains additional residues at its C-terminal region before linking to the phosphatase domain. The varied lengths of the signalling stalk helices might produce altered conformations and orientations of the two connecting functional domains (REC and phosphatase). It is thus important and necessary to elucidate the detailed three-dimensional structure–function relationship of PA3346RS in order to interpret how PA3346RS confers phosphotransfer specificity between HptB and PA3346 as well as downstream domains. A comparison of structures and amino-acid sequences from various receiver domains and stalks is expected to provide more completely distinguishable features. Here, we report the expression, purification, crystallization and X-ray crystallographic characterization of the complete REC domain (127 residues) with the partial stalk linker (36 of 58 residues) of PA3346 (PA3346RS) in order to determine its structure.

2. Materials and methods

2.1. Molecular cloning and protein expression

Recombinant *Escherichia coli* strains carrying plasmids expressing PA3346RS were constructed as described previously (Lin *et al.*, 2006); the forward primer was 5′-GCAGTTGTTCAGGATCCGCT-3′ and the reverse primer was 5′-AATGGGCAAGCTTGTCGAAC-3′. The *PA3346RS* gene was subcloned into the expression plasmid pET30a and subsequently transformed into *E. coli* BL21 (DE3) cells for recombinant protein expression and purification. One colony of the bacteria was picked and placed into 10 ml Luria–Bertani (LB) broth containing kanamycin (50 µg ml^{-1}) at 310 K for overnight incubation. The overnight culture was then transferred into 2 l fresh LB medium containing kanamycin (50 µg ml^{-1}). When the OD_{600} reached 0.6–0.8, isopropyl β-D-1-thiogalactopyranoside (IPTG; final concentration 0.1 m*M*) was added to the culture for induction; incubation was continued for 20 h with rotary shaking and cooling to 293 K. The cells were harvested by centrifugation at 8000 rev min^{-1} at 277 K for 30 min.

2.2. Protein purification

The supernatant medium was discarded and the cell pellet was resuspended in 30 ml binding buffer consisting of 0.3 *M* NaCl, 20 m*M* imidazole and 50 m*M* Tris–HCl pH 8.0 and subjected to cell disruption by ultrasonication using a pulsation cycle of 1 s on and 5 s off with a total duration of 5 min sonication at 40% energy on ice. The soluble protein extract was then collected by centrifugation (18 000 rev min^{-1}) at 277 K for 30 min and passed through an Ni^{2+}–NTA column (length 10 cm; GE Healthcare) pre-equilibrated with 50 ml binding buffer (0.3 *M* NaCl, 50 m*M* Tris–HCl pH 8.0). The column was washed with 100 ml binding buffer containing 40 m*M* imidazole; the purified protein was eluted with 100 ml portions of binding buffer containing imidazole at stepwise-increasing concentrations of 60, 100 and 500 m*M*. The eluted fractions were collected and analyzed by SDS–PAGE. The purified protein was dialyzed in 50 m*M* Tris–HCl buffer pH 8.0 and passed through a column (Q Sepharose High Performance, GE Healthcare) which was eluted with a linear ionic strength gradient (0–1 *M* NaCl, 50 m*M* Tris–HCl pH 8.0). The protein sample was concentrated on a Centricon (10 000 molecular-weight cutoff; Amicon Ultra, Millipore) before crystallization. The yield of the protein was approximately 10 mg ml^{-1}; the purity was greater than 95% as analysed by SDS–PAGE (12%) with Coomassie Brilliant Blue R-250 staining (Fig. 2).

2.3. Protein crystallization

Prior to crystallization trials, the purified PA3346RS protein was prepared and concentrated to 10 mg ml^{-1} in 50 m*M* Tris–HCl buffer pH 8.0. Crystallization was performed in VDX 48-well plates using Crystal Screen kits (Hampton Research) and the hanging-drop vapour-diffusion method at 291 K.

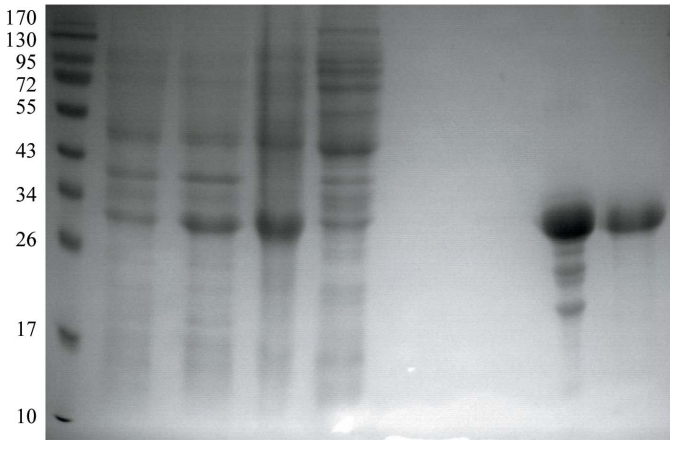

Figure 2
Determination of the purity of PA3346RS. Coomassie Blue-stained SDS–PAGE of pools from expression and purification of PA3346RS. All samples were boiled at 373 K for 10 min in 5× sample buffer. Lane 1, pool from supernatant without IPTG induction; lane 2, pool from supernatant with IPTG (0.1 m*M*) induction; lane 3, pool from supernatant after sonication; lane 4, pool from flowthrough; lane 5, pool from 60 m*M* imidazole wash; lane 6, pool from 100 m*M* imidazole wash; lane 7, pool from 500 m*M* imidazole wash; lane 8, pool from 400 m*M* NaCl elution through a Q Sepharose column; lane *M*, molecular-weight markers (labelled in kDa).

2.4. X-ray data collection and processing

The protein crystals were initially tested and characterized using synchrotron X-rays on beamlines BL13B1 and BL13C1 equipped with CCD detectors (Q315r, ADSC) at the National Synchrotron Radiation Research Center (NSRRC), Taiwan and on beamline BL12B2 equipped with a CCD detector (Q210r, ADSC) at SPring-8, Japan. The crystal was transferred from a crystallization drop into 5 µl cryoprotectant solution consisting of 12%(*v*/*v*) ethanol, 0.15 *M* $MgCl_2$ and 20%(*v*/*v*) glycerol in 0.1 *M* imidazole buffer pH 8.0 for a few seconds, mounted on a synthetic nylon loop (0.3–0.4 mm; Hampton Research) and flash-cooled in liquid nitrogen. For complete data collection, a total 195° of rotation with 0.5° oscillations was measured using an X-ray wavelength of 1.00 Å with an exposure duration of 2 s and a crystal-to-detector distance of 190 mm at 110 K in a nitrogen stream provided by a cryosystem (X-Stream, Rigaku/MSC Inc.). All data were indexed, integrated and scaled using the *HKL*-2000 program suite (Otwinowski & Minor, 1997).

3. Results and discussion

The recombinant N-terminal regulatory region of PA3346, comprising the complete REC domain (127 residues), a partial stalk domain (36 of 58 residues) and His-tag fusion tags at both the N-terminus (52 residues) and the C-terminus (13 residues), was purified using Ni^{2+}–NTA and Q-Sepharose ion-exchange columns (Fig. 2). Under SDS denaturing and reducing conditions the protein showed a single band corresponding to a molecular mass of about 25 000 Da on SDS–PAGE (Fig. 2), which is in agreement with that predicted for recombinant PA3346RS. Small crystals were first observed from a screening condition consisting of 15%(*v*/*v*) ethanol and 0.2 *M* magnesium chloride in 0.1 *M* imidazole buffer pH 8.0 (Wizard I screen condition No. 23; Emerald BioSystems) within one week of initial crystallization setup. During optimization of the crystallization conditions, we found that the presence of Mg^{2+} contributed effectively to crystal growth, perhaps because of its role as a cofactor of the protein. This condition was further refined to produce larger crystals using 2 µl hanging drops consisting of equal volumes (1 µl) of protein solution and reservoir solution, which were equilibrated against 200 µl reservoir solution consisting of 12%(*v*/*v*) ethanol and 0.15 *M* $MgCl_2$ in 0.1 *M* imidazole buffer pH 8.0. Protein crystals appeared after one week and continued to grow to final dimensions of 0.2 × 0.2 × 0.3 mm within one month in an incubator at 291 K. Crystals of satisfactory quality were identified through careful screening and selection for data collection (Fig. 3), as they typically exhibited a fairly high mosaicity (>1.5°). Radiation damage was observed after protracted exposure during data collection, which caused a decrease in $\langle I/\sigma(I)\rangle$ and an increase in $R_{\rm merge}$. Although data were collected for a total rotation of 270°, after inspection of the data statistics with regard to crystal decay we selected only the first 195° range for data processing. Analysis of the diffraction pattern indicated that these crystals exhibited primitive tetragonal symmetry; systematic absences indicated the space group to be $P4_1$ or $P4_3$. Assuming the presence of two molecules per asymmetric unit, the Matthews coefficient was estimated to be 2.39 $Å^3\,Da^{-1}$, corresponding to a solvent content of 48.6% (Matthews, 1968), which is within the general range for protein crystals. Table 1 presents the details of the data statistics.

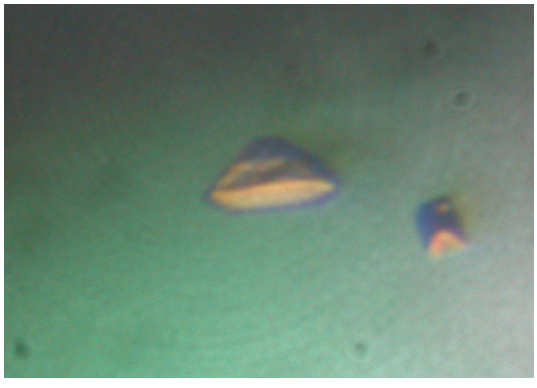

Figure 3
Single crystals of PA3346RS grown by the hanging-drop vapour-diffusion method.

Table 1
Diffraction statistics for the PA3346RS crystal.

Values in parentheses are for the highest resolution shell.

Wavelength (Å)	1.00
Beamline	BL13B1, NSRRC
Temperature (K)	110
Resolution range (Å)	30.0–2.0 (2.07–2.00)
Space group	$P4_1$ or $P4_3$
Unit-cell parameters (Å)	a = 82.38, c = 73.34
Unique reflections	33298
Completeness (%)	97.4 (85.3)
$\langle I/\sigma(I)\rangle$	45.2 (4.6)
Average multiplicity	7.8
$R_{\rm merge}$† (%)	3.8 (36.1)
Mosaicity (°)	0.80
No. of molecules per asymmetric unit	2
Matthews coefficient ($Å^3\,Da^{-1}$)	2.39
Solvent content (%)	48.6

† $R_{\rm merge} = \sum_{hkl}\sum_i |I_i(hkl) - \langle I(hkl)\rangle| / \sum_{hkl}\sum_i I_i(hkl)$, where $I_i(hkl)$ is the ith observation of reflection hkl and $\langle I(hkl)\rangle$ is the weighted average intensity for all observations i of reflection hkl.

Initial attempts to solve the crystal structure of PA3346RS by molecular replacement were performed using the monomer structures of the receiver domain of RssB (sequence identity of 30.1% with 8.4% gaps; PDB entry 3eq2) and WspR (sequence identity of 21.6% with 6.8% gaps; PDB entry 3bre), but all calculations failed to yield an obvious solution. Owing to the low sequence identities and the presence of several gaps in the sequence alignment, the structure of PA3346RS is expected to differ markedly from the available structures. A search for useful heavy-atom derivatives and the preparation of SeMet derivatives for *ab initio* phasing and structure determination is in progress.

We are indebted to Yuch-Cheng Jean and the supporting staff at beamlines BL13B1 and BL13C1 of the National Synchrotron Radiation Research Center (NSRRC), Taiwan and Masato Yoshimura and Hirofumi Ishii at the Taiwan-contracted beamline BL12B2 of SPring-8, Japan for technical assistance. This work was supported in part by grants from the National Science Council (NSC 98-2311-B-213-MY3) and the National Synchrotron Radiation Center (NSRRC 993RSB02 and 1003RSB02) to CJC.

References

Bougdour, A., Wickner, S. & Gottesman, S. (2006). *Genes Dev.* **20**, 884–897.
Bourret, R. B. (2010). *Curr. Opin. Microbiol.* **13**, 142–149.
De, N., Pirruccello, M., Krasteva, P. V., Bae, N., Raghavan, R. V. & Sondermann, H. (2008). *PLoS Biol.* **6**, e67.
Hsu, J.-L., Chen, H.-C., Peng, H.-L. & Chang, H.-Y. (2008). *J. Biol. Chem.* **283**, 9933–9944.
Lin, C.-T., Huang, Y.-J., Chu, P.-H., Hsu, J.-L., Huang, C.-H. & Peng, H.-L. (2006). *Res. Microbiol.* **157**, 169–175.
Matthews, B. W. (1968). *J. Mol. Biol.* **33**, 491–497.
Otwinowski, Z. & Minor, W. (1997). *Methods Enzymol.* **276**, 307–326.

Rodrigue, A., Quentin, Y., Lazdunski, A., Méjean, V. & Foglino, M. (2000). *Trends Microbiol.* **8**, 498–504.
Searls, T., Chen, X., Allen, S. & Yudkin, M. D. (2004). *J. Bacteriol.* **186**, 3195–3201.
Shi, L. (2004). *Front. Biosci.* **9**, 1382–1397.
Stover, C. K. *et al.* (2000). *Nature (London)*, **406**, 959–964.
Varughese, K. I. (2002). *Curr. Opin. Microbiol.* **5**, 142–148.
Varughese, K. I., Tsigelny, I. & Zhao, H. (2006). *J. Bacteriol.* **188**, 4970–4977.
West, A. H. & Stock, A. M. (2001). *Trends Biochem. Sci.* **26**, 369–376.
Wise, A. A. & Price, C. W. (1995). *J. Bacteriol.* **177**, 123–133.
Xu, Q., Porter, S. W. & West, A. H. (2003). *Structure*, **11**, 1569–1581.
Zapf, J., Sen, U., Madhusudan, Hoch, J. A. & Varughese, K. I. (2000). *Structure*, **8**, 851–862.